

## Structural analysis of high-rise reinforced concrete building structures during construction

Xiaobin Song<sup>1a</sup>, Xianglin Gu<sup>\*1</sup>, Weiping Zhang<sup>1b</sup>, Tingshen Zhao<sup>2c</sup> and Xianyu Jin<sup>3d</sup>

<sup>1</sup>Department of Building Engineering, Tongji University, 1239 Siping Road, Shanghai, 200092, P.R. China

<sup>2</sup>Department of Civil Engineering, Huazhong University of Science and Technology, 1037 Luoyu Road, Wuhan, 430074, P.R. China

<sup>3</sup>Department of Civil Engineering, Zhejiang University, 388 Yuhangtang Road, Hangzhou, 310058, P.R. China

(Received October 28, 2009, Accepted August 10, 2010)

**Abstract.** This paper presents a three-dimensional finite element method based structural analysis model for structural analysis of reinforced concrete high-rise buildings during construction. The model considered the time-dependency of the structural configuration and material properties as well as the effect of the construction rate and shoring stiffness. Uniaxial compression tests of young concrete within 28 days of age were conducted to establish the time-dependent compressive stress-strain relationship of concrete, which was then used as input parameters to the structural analysis model. In-situ tests of a RC high-rise building were conducted, the results of which were used for model verification. Good agreement between the test results and model predictions was achieved. At the end, a parametric study was conducted using the verified model. The results indicated that the floor position and construction rate had significant effect on the shore load, whereas the influence of the shore removal timing and shore stiffness have much smaller. It was also found that the floors are more prone to cracking during construction than is ultimate bending failure.

**Keywords:** high-rise building; reinforced concrete structure; construction safety; young concrete; time-dependent analysis.

---

### 1. Introduction

Previous studies on the failures of reinforced concrete (RC) buildings indicated that around 50% of the failures occurred during construction period (Hadipriono and Wang 1986, Eldukair and Ayyub 1991). This is mainly because the fact that concrete is only partially hardened during the construction period and the RC members may be overloaded under the construction load, which would be safely resisted by fully hardened RC members. The current use of fast construction techniques places additional pressure on constructors, who consequently tend to reduce the time

---

\*Corresponding author, Professor, E-mail: [gxl@tongji.edu.cn](mailto:gxl@tongji.edu.cn)

<sup>a</sup>Assistant Professor, E-mail: [xiaobins@tongji.edu.cn](mailto:xiaobins@tongji.edu.cn)

<sup>b</sup>Associate Professor, E-mail: [Weiping\\_zh@tongji.edu.cn](mailto:Weiping_zh@tongji.edu.cn)

<sup>c</sup>Professor, E-mail: [tszhao@mail.hust.edu.cn](mailto:tszhao@mail.hust.edu.cn)

<sup>d</sup>Professor, E-mail: [xianyu@zju.edu.cn](mailto:xianyu@zju.edu.cn)

between the castings of successive floors (Epaarachchi *et al.* 2002).

The stiffness and load carrying capacity of RC structural members during construction has not been fully understood. Much work has been done on the mechanical properties of young/early-age concrete (Gardner and Sau 1986, Klieger 1958, Oluokun *et al.* 1991, Parsons and Naik 1985, Plowman 1956, Zhu 1996). These studies are pertinent to the determination of the stiffness and load carrying capacity of RC members; however they were mostly focused on the strength and modulus of elasticity, whereas the complete stress-strain relationship of young/early-age concrete was neglected.

The load distribution of the high-rise RC buildings during construction has not been fully studied either. Grundy and Kabaila (1963) proposed the simplified method to analyze the load distribution, which has been improved into the refined method (Liu *et al.* 1985), equivalent frame method (Stivaros and Halvorsen 1991) and improved method (Duan and Chen 1986). Fang *et al.* (2001a) proposed a method to obtain the load distribution based on the concept of load redistribution suggested by Mossallam and Chen (1991). The method was verified based on on-site test data (Fang *et al.* 2001b). Kwak and Kim (2006) considered the influence of the time-dependent deformation and construction sequence on the load distribution of the RC frame structures. Chen *et al.* (2006) proposed a strategy to improve the computational efficiency of the construction sequence analysis of high-rise buildings during construction. Most of these methods were basically two dimensional and were originally developed for flat plate construction, and thus may not be adequate for frame construction or structures with irregular plan layout.

This paper presents a three-dimensional finite element method (FEM) based model to analyze the RC high-rise buildings of frame structure during construction. The model consisted of FEM based elements with consideration of the time-dependent properties of concrete and the contribution of the reinforcement as well as the forms. The influence of the construction rate and shore stiffness was also incorporated in the model. Uniaxial compression tests of young concrete and in-situ tests of a RC high-rise building during construction were conducted to provide input parameters and verification to the developed model. Good agreement was achieved. A parametric study was conducted using the verified model to further identify the influence of the floor position, construction rate, shore removal timing, and shore stiffness on the shore load and the safety of the buildings.

## 2. Uniaxial compression tests of young concrete

Uniaxial compression tests of young concrete within 28 days of age were conducted to establish the time-dependent stress-strain relationship of concrete. Two types of concrete composition (as listed in Table 1), with the expected cubic compression strength being 30 MPa and 50 MPa, respectively, were considered. The two strength values are corresponding to the Chinese concrete

Table 1 Concrete composition (content kg/m<sup>3</sup> concrete)

Class	w/c	Water	Cement	Sand	Aggregate
C30	0.4	164	410	634	1276
C50	0.39	219	562	518	1171

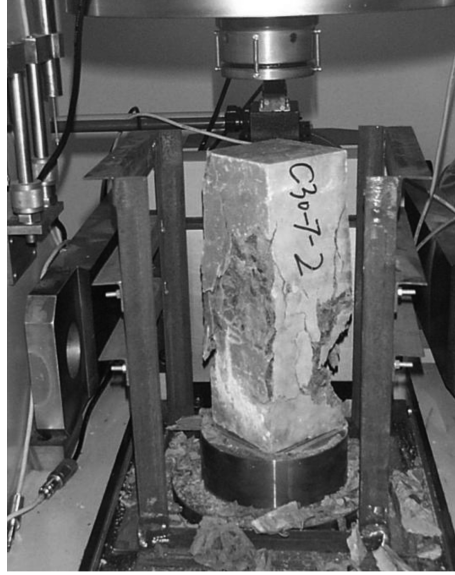


Fig. 1 Test setup for uniaxial compression tests of young concrete

classes C30 and C50 and are most commonly used in construction of RC high-rise buildings in China nowadays.

For each type of concrete composition, twenty-four prismatic specimens were made and tested in six groups (each with four specimens) at ages of 3, 5, 7, 14, 21, and 28 days, respectively. The specimens were of  $100 \times 100 \times 300$  mm and were cast using steel moulds, which were removed after the final setting of the concrete. The specimens were then cured at 100% humidity and  $21.2 \pm 0.5^\circ\text{C}$  to the prescribed age of testing. A RMT-150B rock mechanical testing machine was used to test the specimens under displacement control, of which the loading rate was 0.002 mm/s. The test setup is shown in Fig. 1.

The test results of various concrete ages were used to establish the relationship between the age of the concrete and the corresponding compressive strength,  $f_c(t)$ . This is usually done by fitting the test results to a prescribed mathematic form (Parsons and Naik 1985, for example). In this study the least square method was used for the fitting analysis. The so-obtained time dependent compressive strength can be expressed as

$$f_c(t) = 0.5f_{c,28}t^{0.22} \quad (1)$$

where  $f_{c,28}$  is the compressive strength of concrete measured at 28 days of age,  $t$  is the concrete age, measured in days.

Similarly, the time-dependent modulus of elasticity,  $E_c(t)$ , the strain corresponding to the compressive strength,  $\varepsilon_o(t)$ , and the ultimate strain,  $\varepsilon_u(t)$ , can be expressed as

$$\begin{aligned} E_c(t) &= 0.385E_{c,28}t^{0.29} \\ \varepsilon_o(t) &= \varepsilon_{o,28}(-0.12\ln t + 1.4) \\ \varepsilon_u(t) &= \varepsilon_{u,28}(-0.15\ln t + 1.5) \end{aligned} \quad (2)$$

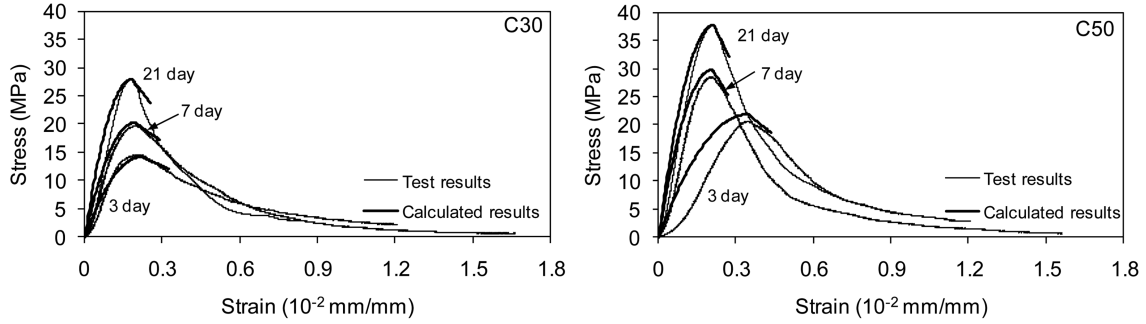


Fig. 2 Test and calculation results of the stress-strain relationship of young concrete

where  $\varepsilon_u(t)$  is the strain on the falling branch of the stress-strain curve corresponding to 85% of the compressive strength,  $E_{c,28}$ ,  $\varepsilon_{o,28}$  and  $\varepsilon_{u,28}$  are the properties measured from concrete of 28 days of age.

The stress-strain relationship of young concrete under compression can then be established based on the time dependent properties in Eqs. (1) and (2). In this study, the mathematic model of the relationship was established based on Hognestad's work (1951), while the constant parameters (strength, modulus of elasticity, etc.) in his model were replaced by the time-dependent expressions in Eqs. (1) and (2) as

$$\sigma_c(t) = \begin{cases} 0.5f_{c,28}t^{0.22} \left[ \frac{2\varepsilon}{\varepsilon_{o,28}(-0.12\ln t + 1.4)} - \frac{\varepsilon^2}{(\varepsilon_{o,28}(-0.12\ln t + 1.4))^2} \right], & \varepsilon \leq \varepsilon_o(t) \\ 0.5f_{c,28}t^{0.22} \left[ 1 - \frac{0.15(\varepsilon - \varepsilon_{o,28}(-0.12\ln t + 1.4))}{(\varepsilon_{u,28}(-0.15\ln t + 1.5) - \varepsilon_{o,28}(-0.12\ln t + 1.4))} \right], & \varepsilon_o(t) < \varepsilon \leq \varepsilon_u(t) \end{cases} \quad (3)$$

The test results of the stress-strain relationship of concrete at different ages and the calculation results using Eq. (3) are shown in Fig. 2. For clarity, only the results of concrete at age of 3, 7, and 21 days are presented.

### 3. Stiffness and load carrying capacity of RC members during construction

Knowing the stress-strain relationship, the stiffness and load carrying capacities of RC members during construction can be fully determined. In previous studies the concrete was normally assumed linear elastic and the contribution of the reinforcing bars were ignored (Epaarachchi *et al.* 2002, Grundy and Kabaila 1963, Liu *et al.* 1985, Stivaros and Halvorsen 1991, Duan and Chen 1986). This is acceptable for flat plate construction, where punching shear failure is the critical mode of failure (Epaarachchi *et al.* 2002). For frame construction where different amount of reinforcement are used in the columns, beams and slabs, the distribution of loads and failure modes may be affected and the calculation of the stiffness and load carrying capacity should include the contribution of the reinforcement.

The stiffness matrix,  $k^e$ , of a three-dimensional FEM-based beam/column element can be expressed as

$$K^e = \begin{bmatrix} \frac{EA}{l} & 0 & 0 & 0 & 0 & 0 & -\frac{EA}{l} & 0 & 0 & 0 & 0 & 0 \\ \frac{12EI_z}{l^3} & 0 & 0 & 0 & \frac{6EI_z}{l^2} & 0 & -\frac{12EI_z}{l^3} & 0 & 0 & 0 & \frac{6EI_z}{l^2} \\ \frac{12EI_y}{l^3} & 0 & -\frac{6EI_y}{l^2} & 0 & 0 & 0 & -\frac{12EI_y}{l^3} & 0 & -\frac{6EI_y}{l^2} & 0 & 0 \\ \frac{GJ}{l} & 0 & 0 & 0 & 0 & 0 & 0 & -\frac{GJ}{l} & 0 & 0 & 0 \\ \frac{4EI_y}{l} & 0 & 0 & 0 & 0 & \frac{6EI_y}{l^2} & 0 & \frac{2EI_y}{l} & 0 & 0 & 0 \\ \frac{4EI_z}{l} & 0 & -\frac{6EI_z}{l^2} & 0 & 0 & 0 & 0 & 0 & \frac{2EI_z}{l} & 0 & 0 \\ \text{symmetric} & & & & & & \frac{EA}{l} & 0 & 0 & 0 & 0 \\ & & & & & & \frac{12EI_z}{l^3} & 0 & 0 & 0 & -\frac{6EI_z}{l^2} \\ & & & & & & \frac{12EI_y}{l^3} & 0 & \frac{6EI_y}{l^2} & 0 & 0 \\ & & & & & & \frac{GJ}{l} & 0 & 0 & 0 & 0 \\ & & & & & & \frac{4EI_y}{l} & 0 & 0 & 0 & 0 \\ & & & & & & \frac{4EI_z}{l} & 0 & 0 & 0 & 0 \end{bmatrix} \quad (4)$$

where  $EA$ ,  $EI_y$ ,  $EI_z$ , and  $GJ$  are the axial, flexural and torsional stiffness, respectively, and are functions of concrete age. To calculate these properties with consideration of the reinforcement and formwork, two assumptions were made: 1) perfect bonding exists between the concrete and the

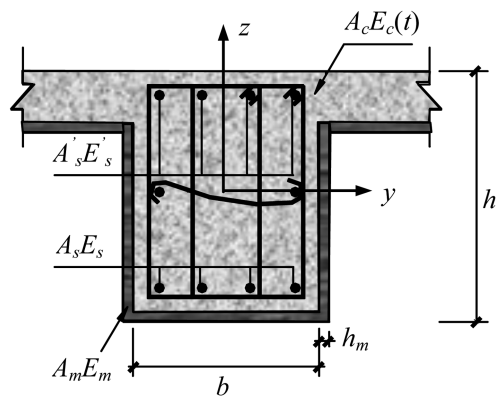


Fig. 3 A RC beam with wood mold

reinforcement shortly after concrete setting; and 2) no bonding exists between the concrete and the formwork. The stiffness of the RC members can then be evaluated based on the principle of superposition. Take the beam in Fig. 3 as an example, the flexural stiffness around  $y$  axis,  $E(t)I_y(t)$ , can be calculated by

$$E(t)I_y(t) = \begin{cases} E_s I_{ys} + E_m I_{ym}, & \text{If } E_c(t) = 0 \\ E_c(t)I_{yc} + E_s I_{ys} + E_m I_{ym}, & \text{If } E_c(t) \neq 0 \end{cases} \quad (5)$$

where  $E_c(t)$ ,  $E_s I_{ys}$  and  $E_m I_{ym}$  are the modulus of elasticity of the concrete, the flexural stiffness of the reinforcement and the forms around  $y$  axis, respectively.

The load carrying capacities of RC high-rise buildings of most concern include the punching shear resistance and the bending capacity of flat plate and frame constructions, respectively. In this study, the punching shear resistance of young concrete members was calculated in the same way as for the fully hardened RC members. The bending capacities, including the cracking moment and the bearing capacity (ultimate moment), on the other hand, were calculated by discretizing the member cross-section into small segments. In this way the locations of the reinforcement can be incorporated in the calculation. The contribution of the forms was considered by simply adding the bending capacity of the forms to the concrete members. For example, the cracking moment and bearing capacity of a RC member with forms can be calculated as

$$\begin{aligned} M_{cr} &= M_{cr,c} \left( 1 + \frac{E_m I_m}{E(t)I} \right) \\ M_u &= M_{u,c} + M_{u,m} \end{aligned} \quad (6)$$

where  $M_{cr}$  and  $M_u$  are the cracking moment and bearing capacity, respectively, of the RC member with the forms;  $M_{cr,c}$  and  $M_{u,c}$  are those of the RC member itself,  $M_{u,m}$  is the bearing capacity of the forms; and  $E_m I_m$  and  $E(t)I$  are the flexural stiffness of the forms and the RC member, respectively.

#### 4. Time-dependent FEM-based model of RC high-rise buildings

The time-dependent model of RC high-rise buildings was aimed at analyzing the load distribution amongst the RC members and the shore system and thus evaluating the safety of the structure. The model was developed based on following assumptions:

- The stiffness and load carrying capacity of the RC members are constant at a given age of concrete;
- The shores behave linear elastic and are pin-connected to the RC members above and underneath;
- The foundation is rigid compared to the concrete slabs;
- The concrete shrinkage and creep are ignorable.

At any given instant during the construction period, the RC columns and beams of the finished part of the RC building were modeled by three-dimensional beam elements, of which the stiffness and load carrying capacities were evaluated using the methodology presented in previous sections. The RC slabs were first divided into strips along the direction of the joists and then further divided along the direction of the girders. For simplicity, the interaction amongst the slab strips along the direction of the joists was ignored. Each slab segment was modeled by a three-dimensional beam

element. The shores were modeled by bar elements and were pin-connected to the RC elements. Fig. 4 shows the model for a part of a RC frame structure with two sets of shores during construction.

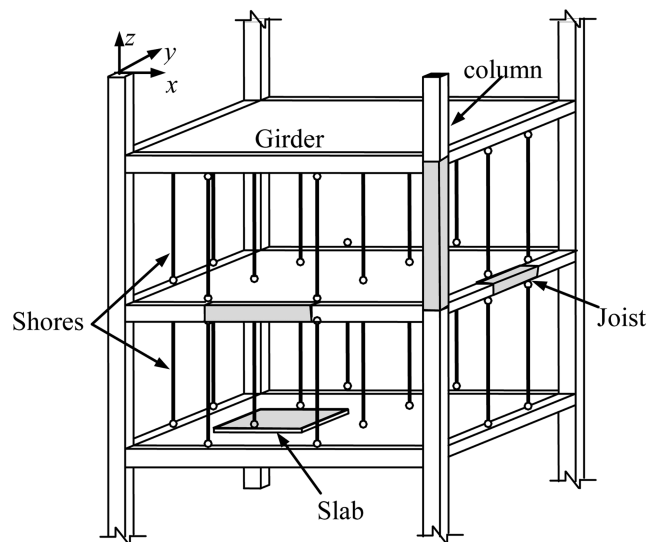


Fig. 4 Three-dimensional FEM-based model of a RC frame structure during construction

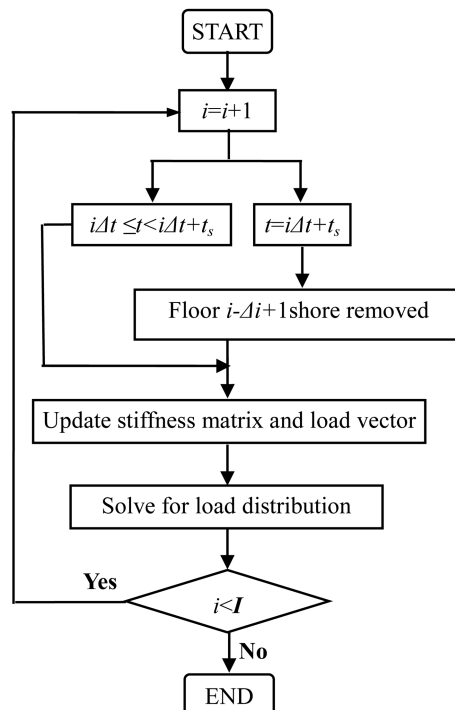


Fig. 5 Flowchart of time-dependent analysis of RC high-rise buildings during construction

With the progressing of the construction, the FEM-based model would have to be updated to reflect the changes in the structural configuration and the concrete properties as well. This was achieved by a set of iterations considering the major operations during the construction of a standard floor: for  $i$ th floor, the concrete is cast at day  $\Delta t(i-1)$ , where  $\Delta t$  is the construction rate and is equal to the number of days used to construct one standard floor; at day  $\Delta t(i-1) + t_s$  the shore system of the lowest shored floor,  $i - \Delta i + 1$ , is removed, where  $t_s$  and  $\Delta i$  are the timing of shore removal and the number of floors shored at the same time, respectively. Thus, at any given instant in time, the concrete ages and the structural configuration can be identified uniquely by  $\Delta t$ ,  $\Delta i$ , and  $t_s$ . The flowchart of the analysis is shown in Fig. 5, where the iteration terminates when the current floor,  $i$ , exceeds the total number of floor,  $I$ , of the building.

## 5. In-situ tests of a RC high-rise building

In-situ tests of a RC frame-and-shear-wall high-rise building during construction were conducted (Zhao 2002). The building is of 21 floors (90.25 m high). The RC columns were constructed using C50 concrete and the beams and floors were constructed using C30 concrete. The modulus of elasticity and the tensile strength of the reinforcement are  $2.0 \times 10^5$  MPa and 210 MPa, respectively. The geometry of the cross-sections of the columns, beams and slabs within the testing areas is listed

Table 2 Cross-sectional dimensions and reinforcement of the RC members (unit: mm)

Member	Dimension	Reinforcement	Stirrup	Concrete protection cover
Column	1000 × 1000	8 $\phi$ 25	$\phi$ 12@100	25
Girder	400 × 600	6 $\phi$ 25	$\phi$ 8@200	25
Joist	250 × 500	6 $\phi$ 25	$\phi$ 8@200	25
Slab strip	110*	$\phi$ 8@200	--	15

\*The width of the slab strip is dependent on its position whereas the depth is constant at 110 mm

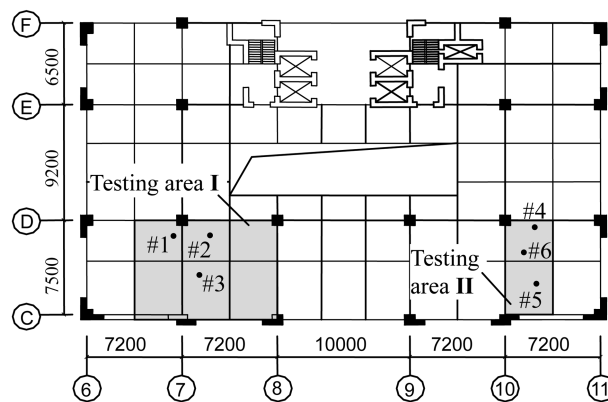


Fig. 6 Plan layout of the standard floor and the testing areas



Fig. 7 Shore load measurement

in Table 2. The plan layout of the standard floor and the location of the testing areas are shown in Fig. 6, in which, testing area **I** is on the 7th floor and testing area **II** is on the 10th floor.

The building was constructed using three sets of shoring systems, i.e., three floors were shored at the same time. The forms were made of nine-ply plywood of 20 mm thick. The shores were made of  $48 \times 3.5$  mm steel pipes with the modulus of elasticity of  $1.82 \times 10^5$  N/mm<sup>2</sup>. The shoring spacing was between 0.8 m and 1.0 m. The shore loads, i.e., the internal force of the shores, were measured by using strain gauges attached onto the surface of the shores, as shown in Fig. 7.

Due to the changes of the construction schedule, the construction rate,  $\Delta t$ , from the 7th floor to the 10th floor (corresponding to the time-history of testing area **I**) was 10 days, whereas for the 11th and higher floors (corresponding to the time-history of testing area **II**),  $\Delta t$  was reduced to 7 days. The timing of the shore removal,  $t_s$ , was kept constant as 1 day after the casting of a new floor.

## 6. In-situ test results and model verification

The FEM model only considered the structural components within the test areas to reduce the computation cost, as shown schematically in Fig. 4. For simplicity, the RC shear walls (as shown in Fig. 6) were modeled as columns with equivalent load carrying capacities. All the columns, beams and slabs were assumed to be rigidly connected to neighboring members. The analysis considered the construction load and the self-weight of the RC members. Based on the in-situ investigation, the construction load during the testing of area **I** was taken as 1.5 kN/m (when casting concrete) and 2.5 kN/m (when removing shores), respectively. The construction load of the testing area **II** was set to be zero since not much load was measured during the testing.

The model predictions and test results of the internal force of the shores (shore load) at certain time instants are listed in Table 3, where the age refers to the concrete age of the beams and slabs (which were cast monolithically). The test results were presented by the averages of the shore loads measured from all the shores within the testing areas, while the represented model predictions were represented by the minimum, maximum and mean values.

It can be seen that the model predictions are in good agreement with the test results. The error is mostly less than 25%, which can be caused by incidental loads or minor changes of construction

Table 3 Model predictions and test results of the shore load (unit:  $D^1$ )

Age (day)	Model			Test (mean)	Test/Model <sup>2</sup>
	Maximum	Minimum	Mean		
<b>Testing area I</b>					
0~1	1.64	0.92	1.25	1.24	0.99
10~11	3.28	0.98	2.06	1.86	0.90
20~21	3.56	0.98	2.11	1.57	0.75
<b>Testing area II</b>					
0~1	1.15	0.83	1.13	1.24	1.10
7~8	2.25	0.79	1.44	1.45	1.01
14~15	2.50	0.75	1.56	1.41	0.90

<sup>1</sup> $D$  is the weight of the slab per square meter  
<sup>2</sup> The model results are based on mean values

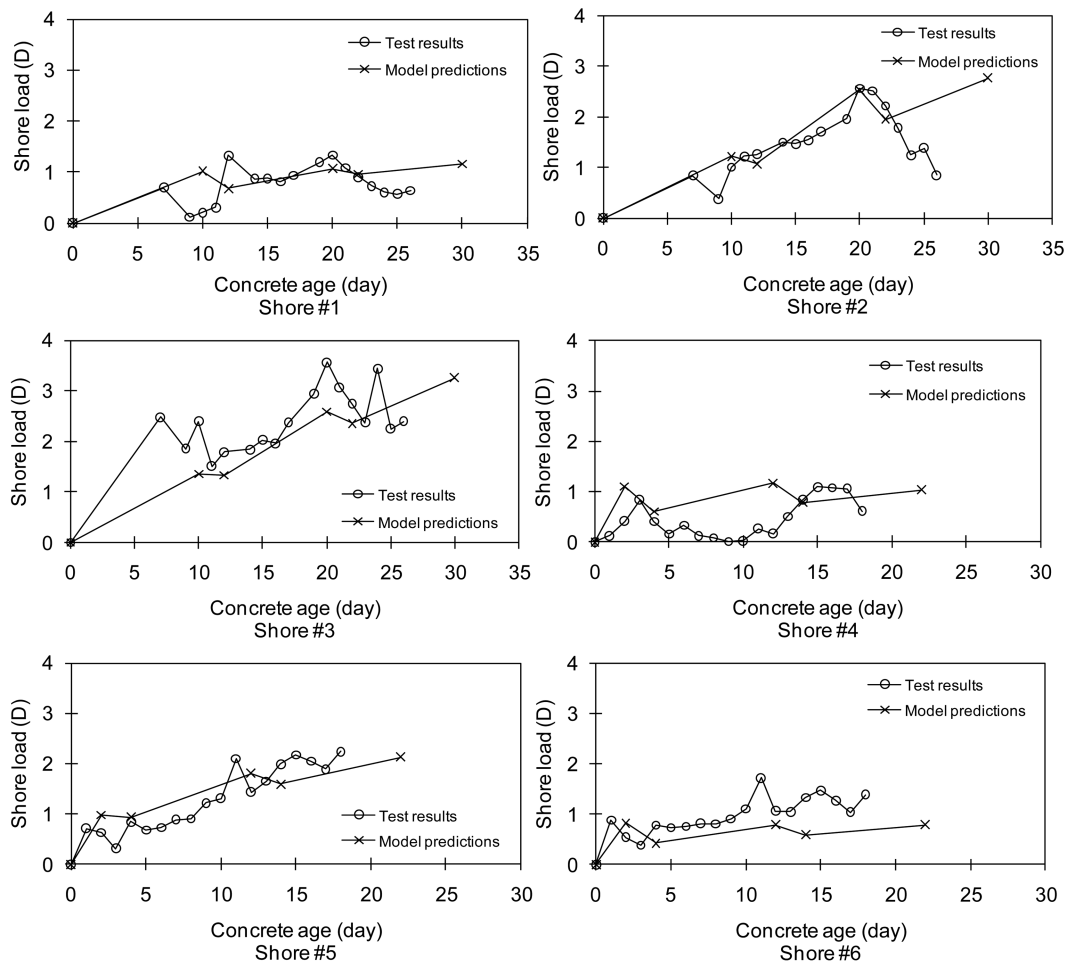


Fig. 8 Test results and model predictions of the time-history of shore load

plan during the testing period.

The model was then further verified based on the shore loads at specific locations, including those beside the girders (#1 and #4) and joists (#3 and #6) and underneath the slabs (#2 and #5), as shown in Fig. 7. The time-history of the shore load from concrete casting to shore removal of the testing area was also identified. The model predictions and the test results are shown in Fig. 8, where  $D$  is the weight of  $1.0 \text{ m}^2$  area of slab.

As can be seen from slab of  $1.0 \text{ m}^2$  area, the model predictions agree well with the test results although the latter turned out to be more fluctuated. This is mainly due to the incidental loadings during the construction process. These incidental loads were not considered in the numerical analysis to reduce the computation cost.

### 7. Parametric study

The in-situ test data were limited to the specific structural configuration and construction plan. The influence of the floor position, construction rate, timing of shore removal and shore stiffness on the shore load as well as the structural safety (i.e., cracking or failure) was not studied due to limited resources. In this study, the verified model was used to conduct a parametric study to identify the influence of the afore-mentioned factors. For simplicity, a six-story  $3.6 \times 4.0 \text{ m}$  RC frame structure was considered. The foundation was assumed to be rigid. The construction rate was assumed as 7 days and the shores were removed 2 days after the casting of a new floor. Three sets of shoring system were used. Steel forms of 3 mm thick and steel pipes of  $48 \times 3.5 \text{ mm}$  were considered. The concrete was assumed to be C30. The plan view of the standard floor and the cross-sectional details of the joists, beams and columns are shown schematically in Fig. 9, whereas the reinforcement of the slab was assumed to be 8 mm in diameter and spaced 200 mm on center in both principle directions of the slabs. The modulus of elasticity, the strength of the reinforcement and the construction loads were assumed to be the same as those used in the testing area II of the in-situ testing study.

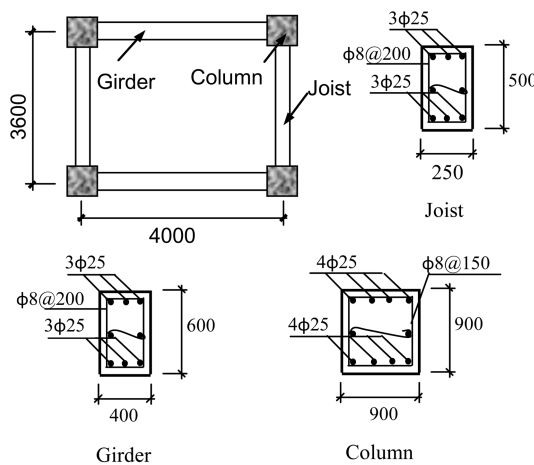


Fig. 9 Details of the cross-sections of the beams and columns of the six-story building

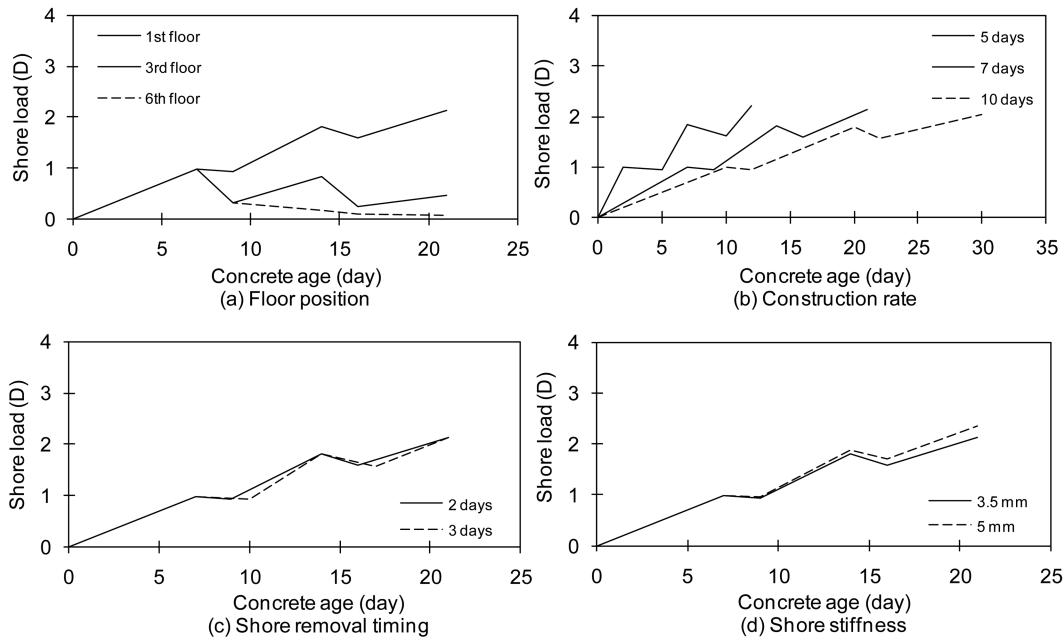


Fig. 10 Influence of floor number, construction speed, time of shore removal and shore stiffness on shore load

## 8. Shore load

The time-history of the average shore load was studied. The shore load was expressed in the ratio to the self-weight of the floor of unit area ( $1.0 \text{ m}^2$ ). The results are shown in Fig. 10, where the results in (a) indicate the influence of the floor positions (the first, third and sixth floors) and the results in (b), (c) and (d) show the influence of the construction rate, timing of shore removal and shore stiffness (characterized by the wall thickness of the shoring pipes) on the shore load of the first floor.

It was found that the shore loads of different floors developed in different ways with respect to the concrete age, as shown in Fig. 10(a): the shore load of the first floor increased with the concrete age and reached maximum before the shores were removed, whereas the shore loads of the third and sixth floors decreased with the concrete age. This is because the shores of the third floor were supported on the second floor which was not as rigid as the foundation and the sixth floor did not have any upper floors.

Fig. 10(b) indicates that increasing the construction rate does not apparently increase the magnitude of the shore load; however, it does bring earlier the maximum shore load which can cause punching shear failure, especially after the slab forms are removed.

Figs. 10(c) and (d) indicate that the timing of shore removal and the shore stiffness do not apparently affect the shore load of the first floor: changing the timing of shore removal only affects the time of occurrence of the shore load while its magnitude is not significantly affected. The shore stiffness does not affect the shore load either until the concrete reaches certain age, after which the ratio between the stiffness of the shores and the stiffnesses of the slabs and beams above becomes pertinent to the load distribution.

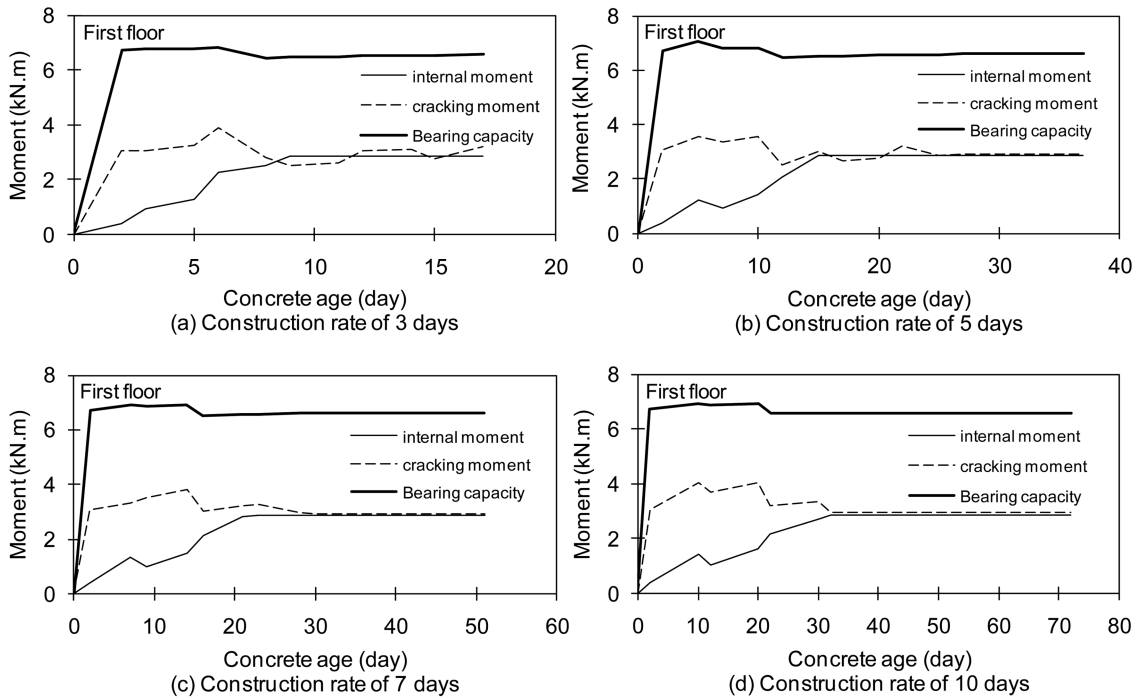


Fig. 11 Safety of the first floor slab under different construction rates

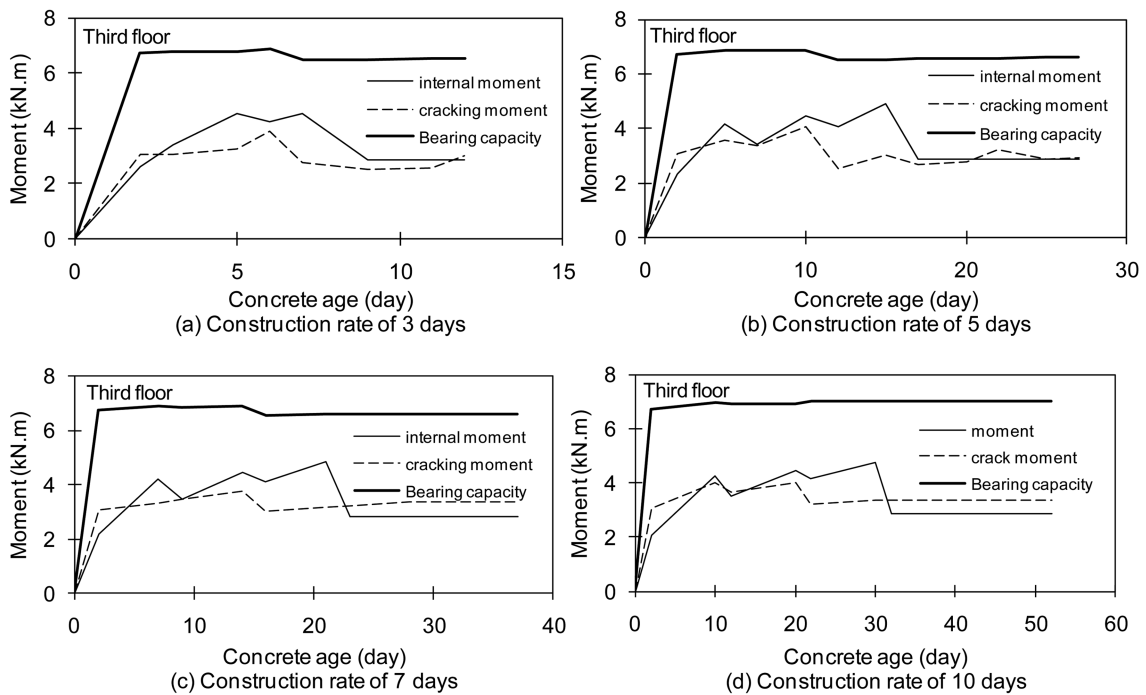


Fig. 12 Safety of the third floor slab under different construction rates

## 9. Structural safety

RC frame structures during construction can have beams and slabs cracked or failed due to overloading. For simplicity, this study was focused on the safety of the floor slabs concerning bending failure. Two major factors, including the floor position (first and third floors) and construction rate (3, 5, 7, and 10 days), were considered. The internal moments obtained from the structural analysis were compared to the cracking moment and bearing capacity, which were calculated using Eq. (6). The results are shown in Figs. 11 and 12, respectively.

It was found that increasing the construction rate may lead to higher risk of floor cracking. Figs. 11 and 12 also indicate that the slab of the third floor is more prone to cracking than that of the first floor. The higher internal moments in the slab of the third floor is caused by the fact that the first floor is shored on top of a rigid foundation, whereas the third floor is shored on the second floor (which is not so rigid). For both floors, cracking is most likely to occur at the moment when the shores are removed. In this study no ultimate bending failure was observed, as can be seen from the comparison of the bearing capacity and the internal moment in Figs. 11 and 12.

## 10. Conclusions

This paper presented a three-dimensional FEM based structural analysis model for RC high-rise buildings during construction. The model considered the time-dependency of the structural configuration and material properties, as well as the construction rate and shoring stiffness. Uniaxial compression tests of young concrete and in-situ test of a RC high-rise building were conducted to provide input parameters and verification to the model. The modeling error of the shore load was found to be less than 25%. The reasons include incidental loads as well as minor changes of construction plan during the testing period, which are beyond the scope of this study.

A parametric study was conducted to further identify the influential factors, from which it was found that the floor position and construction rate have significant effect on the shore load, whereas the influence of the shore removal timing and shore stiffness is immaterial. It was also found that the floors are more prone to cracking rather than ultimate bending failure. The knowledge generated in this study and the developed model can be used as reference in design of construction plan of RC high-rise buildings and therefore contributes to the improvement of their safety level during construction in the long run.

## Acknowledgements

This study is financially supported by National Basic Research Program of China (973 program) (Grant No. 2009CB623200) and National Natural Science Foundation of China (Grant No. 50838008).

## References

Duan, M.Z. and Chen, W.F. (1986), "Design guidelines for safe concrete construction", *Concrete Int.*, **18**(10), 44-

- 49.
- Eldukair, Z.A. and Ayyub, B.M. (1991). "Analysis of recent U.S. structural and construction failures", *J. Perform. Constr. Fac.*, **5**(1), 57-73.
- Epaarachchi, D.C., Stewart, M.G. and Rosowsky, D.V. (2002), "Structural reliability of multistory buildings during construction", *J. Struct. Eng.-ASCE*, **128**(2), 205-213.
- Fang, D.P., Zhu, H.Y., Geng, C.D. and Liu, X.L. (2001), "On-site measurements of structural characteristics of reinforced concrete buildings during construction", *ACI Struct. J.*, **98**(2), 157-163.
- Fang, D.P., Zhu, H.Y., Geng, C.D. and Liu, X.L. (2001), "Structural analysis of reinforced concrete buildings during construction", *ACI Struct. J.*, **98**(2), 149-156.
- Gardner, N.J. and Sau, P.L. (1986), "Strength development and durability of CSA type 30 cement/slag/fly-ash concrete for arctic marine applications", *Durab. Build. Mater.*, **4**(2), 179-200.
- Grundy, P. and Kabaila, A. (1963), "Construction loads on slabs with shored formwork in multistory buildings", *ACI J.*, **60**(12), 1729-1738.
- Hadipriono, F.C. and Wang, H.K. (1986), "Analysis of causes of false-work failures in concrete structures", *J. Constr. Eng. M. ASCE*, **112**(1), 112-121.
- Hognestad, E. (1951), "A study of combined bending and axial load in reinforced concrete members", University of Illinois Engineering Experimental Station, Bulletin Series No.399, 128.
- Klieger, P. (1958), "Effect of mixing and curing temperature on concrete strength", *ACI J. Proceed.*, **29**(12), 1063-1081.
- Kwak, H.G. and Kim, J.K. (2006), "Time-dependent analysis of RC frame structures considering construction sequences", *Build. Environ.*, **41**, 1423-1434.
- Liu, X.L., Chen, W.F. and Bowman, M.D. (1985), "Construction load analysis for concrete structures", *J. Struct. Eng.-ASCE*, **111**(5), 1019-1036.
- Mossallam, K.H. and Chen, W.F. (1991), "Determining shoring loads for reinforced concrete construction", *ACI Struct. J.*, **88**(3), 340-350.
- Oluokun, F.A., Burdette, E.G. and Deatherage, J.H. (1991), "Elastic modulus, poisson's ratio and compressive strength relationships at early ages", *ACI Mater. J.*, **88**(1), 3-10.
- Parsons, T.J. and Naik, T.R. (1985), "Early age concrete strength determination by maturity", *Concrete Int.*, **7**(2), 37-43.
- Plowman, J.M. (1956), "Maturity and strength of concrete", *Mag. Concrete Res.*, **8**(22), 13-22.
- Stivaros, R.C. and Halvorsen, G.T. (1991), "Equivalent frame analysis of concrete buildings during construction", *Concrete Int.*, **13**(8), 57-62.
- Zhao, T.S. (2002), "Safety analysis of R.C. high-rise buildings during construction", Ph.D. Thesis, Department of Building Engineering, Tongji University, Shanghai China. (in Chinese)
- Zhu, B.F. (1996), "Relationship between ultimate tensile strain and tensile and compressive strengths", *China Civil Eng. J.*, **5**, 72-75.
- Chen, P., Li, H., Sun, S.L. and Yuan, M.W. (2006), "A fast construction sequential analysis strategy for tall buildings", *Struct. Eng. Mech.*, **23**(6), 675-689.